Supplement of Biogeosciences, 15, 4661–4682, 2018
https://doi.org/10.5194/bg-15-4661-2018-supplement

Biogeosciences
Open Access

Supplement of

Transport and storage of anthropogenic C in the North Atlantic Subpolar Ocean

Virginie Racapé et al.

Correspondence to: Virginie Racapé (virginie.racape@ifremer.fr)

Supplement

S1. Evaluation of the proxy proposed by Zunino et al. (2014) in ORCA05-PISCES

Zunino et al. (2014) proposed a novel proxy to evaluate processes governing the long term changes of Cant transport in the northern region of the North Atlantic subpolar gyre. This proxy ($T_{Cant}°$) was computed from the intensity of the meridional overturning circulation (MOC) times the difference of averaged-Cant concentrations between the northward flow of warm and saline upper ocean waters, rich in Cant, and the southward return flow of colder and fresher waters across a section (noted *Δ[Cant]*, Eq. (S1)). In this region, the MOC intensity was computed in density coordinates to remove depth overlaps between its upper and lower limbs (Marsh et al., 2005; Lherminier et al., 2007). It was calculated as the integration of volume transport from Greenland to Portugal and from bottom to each density level. Maximum negative value corresponds thus to the net southward transport of the lower MOC; the absolute value of this estimate corresponds to the intensity of the MOC (MOC_σ in Eq. (S1)). In the model, the proxy (${}^{m}T_{Cant}°$) was evaluated from monthly simulations over the period 2002-2010.

$$ {}^{m}T_{CANT}{}^{o} = MOC_{\sigma}\Delta[C_{ANT}] \qquad \text{(S1)} $$

$T_{Cant}°$ was defined by Zunino et al. (2014) as the proxy of the diapycnal component of the advective transport of Cant across the OVIDE section. It could be used in the model if (1) the diapycnal transport of Cant (${}^{m}T_{Cant}{}^{diap}$) is the major mechanism driving changes in Cant advective transport across the OVIDE section and if (2) $T_{Cant}°$ is a good proxy of ${}^{m}T_{Cant}{}^{diap}$.

S1.1. Is ${}^{m}T_{Cant}{}^{diap}$ the major mechanism driving the ${}^{m}T_{CANT}{}^{adv}$ variability?

In the offline approach, the simulated advective transport of Cant ($[{}^{m}T_{Cant}{}^{adv}]^{offline}$) was decomposed in three components along the Greenland-Portugal OVIDE section (Eq. (S2)) to compare with results from Zunino et al. (2014). The approach was initially developed by Bryden and Imawaki (2001) to study heat transport and was recently adapted by Zunino et al. (2014) for Cant advective transport (${}^{m}T_{Cant}{}^{adv}=[{}^{m}T_{Cant}{}^{adv}]^{offline}$). Application of this approach to monthly model output allowed to infer (i) the isopycnal transport of Cant across the OVIDE section, noted ${}^{m}T_{Cant}{}^{iso}$, (ii) the diapycnal transport of Cant (${}^{m}T_{Cant}{}^{diap}$), related to the overturning circulation and (iii) the net transport of Cant (${}^{m}T_{Cant}{}^{net}$), related to the arctic mass balance (Lherminier et al., 2007).

$$\left[{}^{m}T_{Cant}^{adv}\right]^{offline} = {}^{m}T_{Cant}^{adv} = {}^{m}T_{Cant}^{net} + {}^{m}T_{Cant}^{diap} + {}^{m}T_{Cant}^{iso} \qquad \text{(S2)}$$

The decomposition of the advective transport of Cant across the Greenland-Portugal OVIDE section yielded 2002-2010 mean values of diapycnal, isopycnal and net transport of Cant of 178±42 kmol s^{-1}, -97±24 kmol s^{-1} and 13±9 kmol s^{-1} respectively. The sum was equal to ${}^{m}T_{Cant}^{adv}$ and amounts to 94±43 kmol s^{-1}. It's coherent with values computed online from 5 day averages (90±44 kmol s^{-1}). Both estimates (online and offline) are strongly correlated ($r=0.94$, p-value = 0.00; $r^2 = 0.89$, Fig. S1a). In general, the model results were lower than those obtained from observation-based assessments (Table S1). However and as expected, the diapycnal component drives a large northward transport of Cant-rich waters across the section. It is partially compensated by the isopycnal component, yielding a negligible net transport (Fig. S4a). Moreover, the correlation between ${}^{m}T_{Cant}^{adv}$ and each transport component (${}^{m}T_{Cant}^{diap}$, ${}^{m}T_{Cant}^{iso}$ and ${}^{m}T_{Cant}^{net}$) was only significant with the diapycnal component ($r = 0.75$, p-value = 0.00 from all simulations; $r= 0.89$, p-value = 0.00 from June simulations; Fig.S1a). The diapycnal component explain from 60% (full model output over OVIDE period) to 78% (June outputs) of ${}^{m}T_{Cant}^{adv}$ variability. These results attest that the variability of the ORCA05-PISCES advective transport of Cant is controlled by those of the diapycnal component, which validates the first condition to be satisfied in order to use the proxy in the model.

S1.2. Is $T_{Cant}°$ a good proxy of ${}^{m}T_{Cant}^{diap}$?

The mean value of $T_{Cant}°$ derived from model outpus is higher by 155±57 kmol s^{-1} compared with ${}^{m}T_{Cant}^{diap}$, while the difference between the proxy and the diapycnal component estimated by Zunino et al. (2014) is only of 22 kmol s^{-1}. In the model, $T_{Cant}°$ is not equal to ${}^{m}T_{Cant}^{diap}$. This curiosity is probably due to the parametrizations of the two quantities. ${}^{m}T_{Cant}°$ is in fact a proxy of diapycnal transport of Cant based on the assessments of the MOC magnitude times ΔCant between both limbs of the MOC (Eq. (S1)) whereas ${}^{m}T_{Cant}^{diap}$ (Eq. (S2)) is a direct estimation using Cant concentration times velocity of each grid level. The underestimation of the MOC magnitude and ΔCant by the model is not as large as those detected on the volume transport (Fig. 5) and the Cant concentration (Fig. 6) in Sect. 3.1. This implies that the difference between TCant° from model output and TCant° from OVIDE data set (Table S1) is not as large as the model-data differences obtained for T_{Cant}^{diap}. In the model, $T°_{Cant}$ also presents a seasonal cycle with an amplitude higher than 100 kmol s^{-1}, in phase (opposite) with those observed on MOCσ and on ΔCant (Figs. S1b to S1c). This seasonal organization is not detected on $^{m}T_{Cant}^{diap}$ and $^{m}T_{Cant}^{adv}$ (Fig. S1). This is confirmed by the small correlation obtained between the proxy and $^{m}T_{Cant}^{diap}$ (r = 0.18, p-value = 0.04) or between the proxy and $^{m}T_{Cant}^{adv}$ (r = 0.33, p-value = 0.00) over the full period (2002-2010). It should be noted that the correlation between $^{m}T_{Cant}^{\circ}$ and $^{m}T_{Cant}^{diap}$ from June simulations (r=0.66, p-value = 0.03) is comparable with the observations. This is not observed for those estimated between $^{m}T_{Cant}^{\circ}$ and $^{m}T_{Cant}^{adv}$ (r = 0.35, p-value = 0.29). These comments refute thus the second condition to use the estimator to disentangle the effect of both circulation and Cant accumulation variability on the Cant transport variability.

Table S1: Model-data comparison over the period covered by OVIDE cruises (2002-2010). Average and standard deviation (SD) for observation-based estimates (column 2) and model outputs (columns 3 to 5). Model outputs: (1) June average with SD being a measure of interannual variability, (2) average year with SD corresponding to the average seasonal variability, or (3) average over the full period with SD being representative of total variability (interannual + seasonal).

	OVIDE data set	**ORCA05-PISCES**		
		June only	**Average year**	**Full period**
T_{Cant}^{0} (kmol s^{-1})	413.1±70.4	332.0±27.0	338.0±19.2	333.5±50.8
T_{Cant}^{diap} (kmol s^{-1})	391.2±79.2	201.5±30.9	178.2±9.2	178.1±41.8
T_{Cant}^{iso} (kmol s^{-1})	-164.5±16.2	-112.7±13.3	-97.0±7.8	-96.5±24.1
T_{Cant}^{net} (kmol s^{-1})	21.0±17.5	3.6±6.3	13.9±5.4	12.7±8.8
T_{Cant}^{adv} (kmol s^{-1})	247.7±77.3	92.4±32.4	95.1±13.48	94.3±42.6

Fig. S1 : 2002-2012 monthly evolution of (a) the diapycnal (blue), isopycnal (red), net (green) and total (black) transport of Cant and T_{Cant}° (magenta) (kmol s^{-1}), of (b) the magnitude of the MOC (MOCσ, Sv), and of (c) the Cant concentration in the upper (triangles) and the lower (inverse triangles) MOC (µmol kg^{-1}) computed in offline either from model output (continuous line) or from observation-based assessments (dotted line) for the Greenland-Portugal OVIDE section. Colored dots symbolize the month June. On panel (a), time series in grey represents the total transport of Cant computed in online by the model (including advective, diffusive and eddies terms).

S2. Description of section in the model

The sections at 25°N, 36°N, OVIDE or at the sills were collocated in the model as a continuous line between A and B defined by zonal (y) or meridional (x) grid segments. Horizontal velocities ($\vec{u}$ and $\vec{v}$) used to estimate mass transport across a section were towards the North (for $\vec{v}$) if orthogonal to grid segment x and towards the East (for $\vec{u}$) if orthogonal to grid segment y (Fig. S2).

Fig. S2: Schematic representation of section in the model

S3. Online computation of transport of Cant across a section

Fig. S3: Transport of Cant across (from top to bottom) 25° N, 36° N and OVIDE sections computed online by ORCA05-PISCES over the period 2003-2011 (monthly resolution). In the online approach, the transport of Cant (${}^{m}T_{Cant}^{online}$, black bold line) is the sum of the advection (${}^{m}T_{Cant}^{adv}$, red fine line), the diffusion (${}^{m}T_{Cant}^{lf}$, blue fine line) and the eddy (${}^{m}T_{Cant}^{eiv}$, green fine line) contributions. For each section, ${}^{m}T_{Cant}^{adv}$ is the major component of ${}^{m}T_{Cant}^{online}$.

S4. Volume and Cant transported within water classes at 25°N, 36°N and at the OVIDE section.

Fig S4a: Simulated annual time series of Cant and volume transported (Pg yr^{-1}) by the northward (full line) and southward (dashed line) following components of NACW (class 1) through 25°N (green), 36°N (red) and OVIDE (black) over the period 1959-2011.

Fig S4b: Simulated annual time series of Cant and volume transported (Pg yr^{-1}) within IW (class 2) through 25°N (green), 36°N (red), OVIDE (black) and the Greenland-Iceland-Scotland sills (blue) over the period 1959-2011.

Fig S4c: Simulated annual time series of Cant and volume transported (Pg yr^{-1}) within NADW (Class 3) through 25°N (green), 36°N (red), OVIDE (black) and the Greenland-Iceland-Scotland sills (blue) over the period 1959-2011.

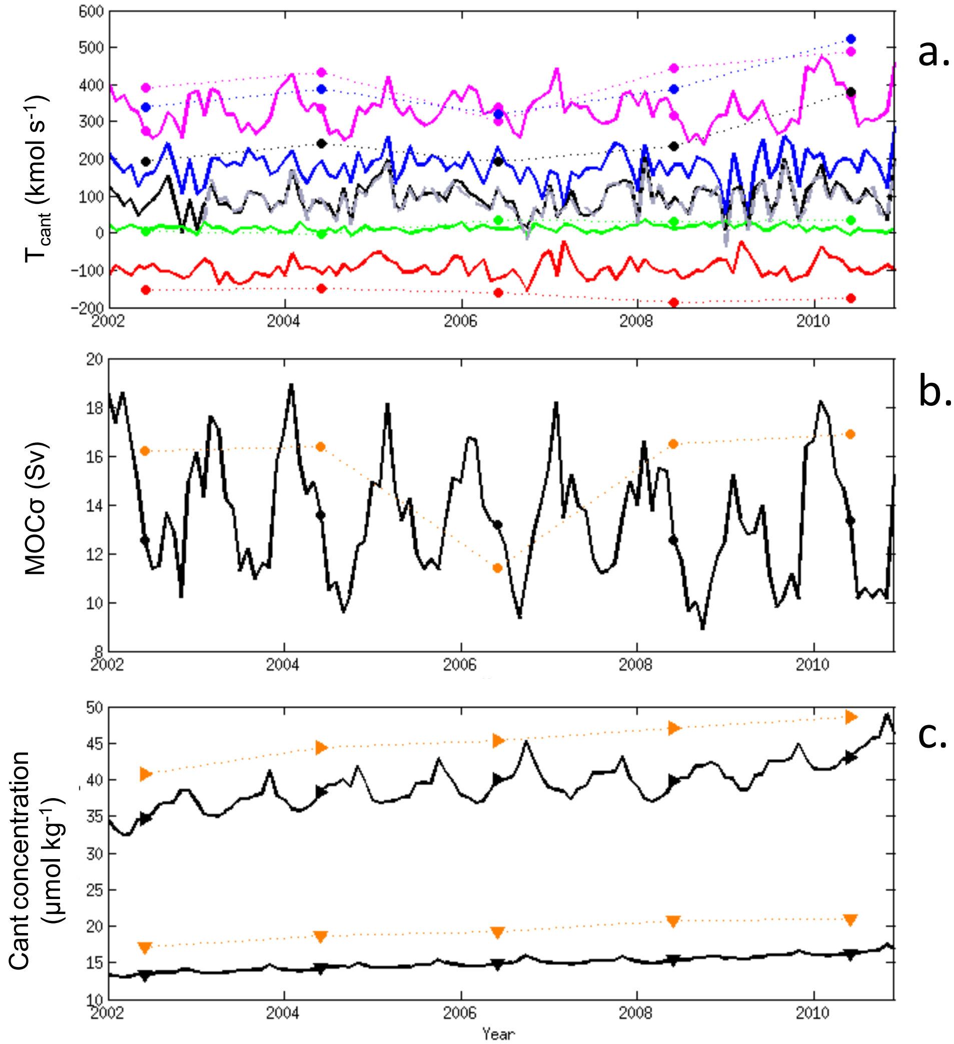

Fig. S1 : 2002-2012 monthly evolution of (a) the diapycnal (blue), isopycnal (red), net (green) and total (black) transport of Cant and TCant° (magenta) (kmol s^{-1}), of (b) the magnitude of the MOC (MOCσ, Sv), and of (c) the Cant concentration in the upper (triangles) and the lower (inverse triangles) MOC (µmol kg-1) computed in offline either frommodel outputs (continuous line) or from observation-based assessments (dotted line) for the Greenland-Portugal OVIDE section. Colored dots symbolize the month June. On panel (a), time series in grey represents the total transport of Cant computed in online by the model (including advective, diffusive and eddies terms).

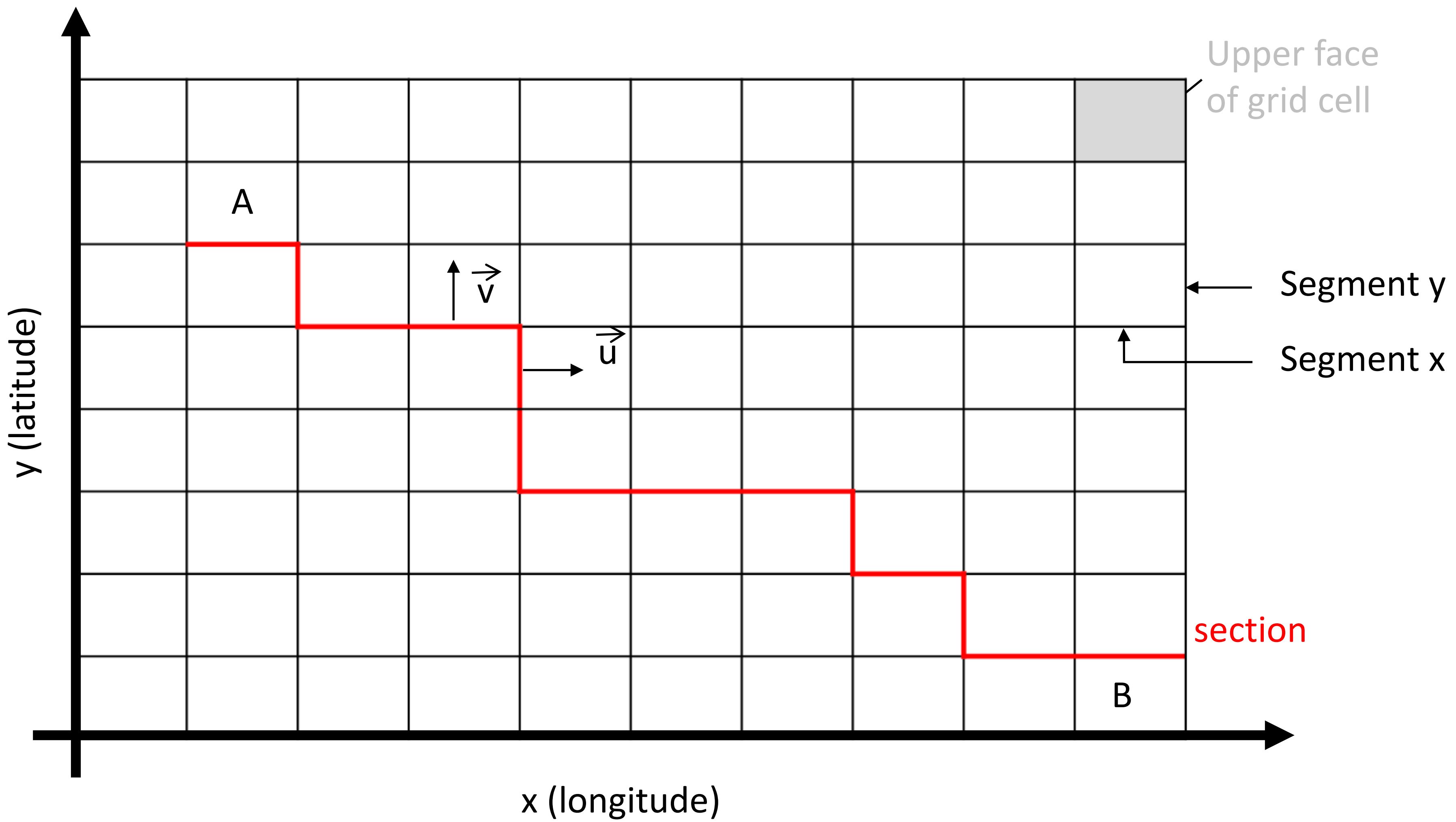

Fig. S2: Schematic representation of section in the model.

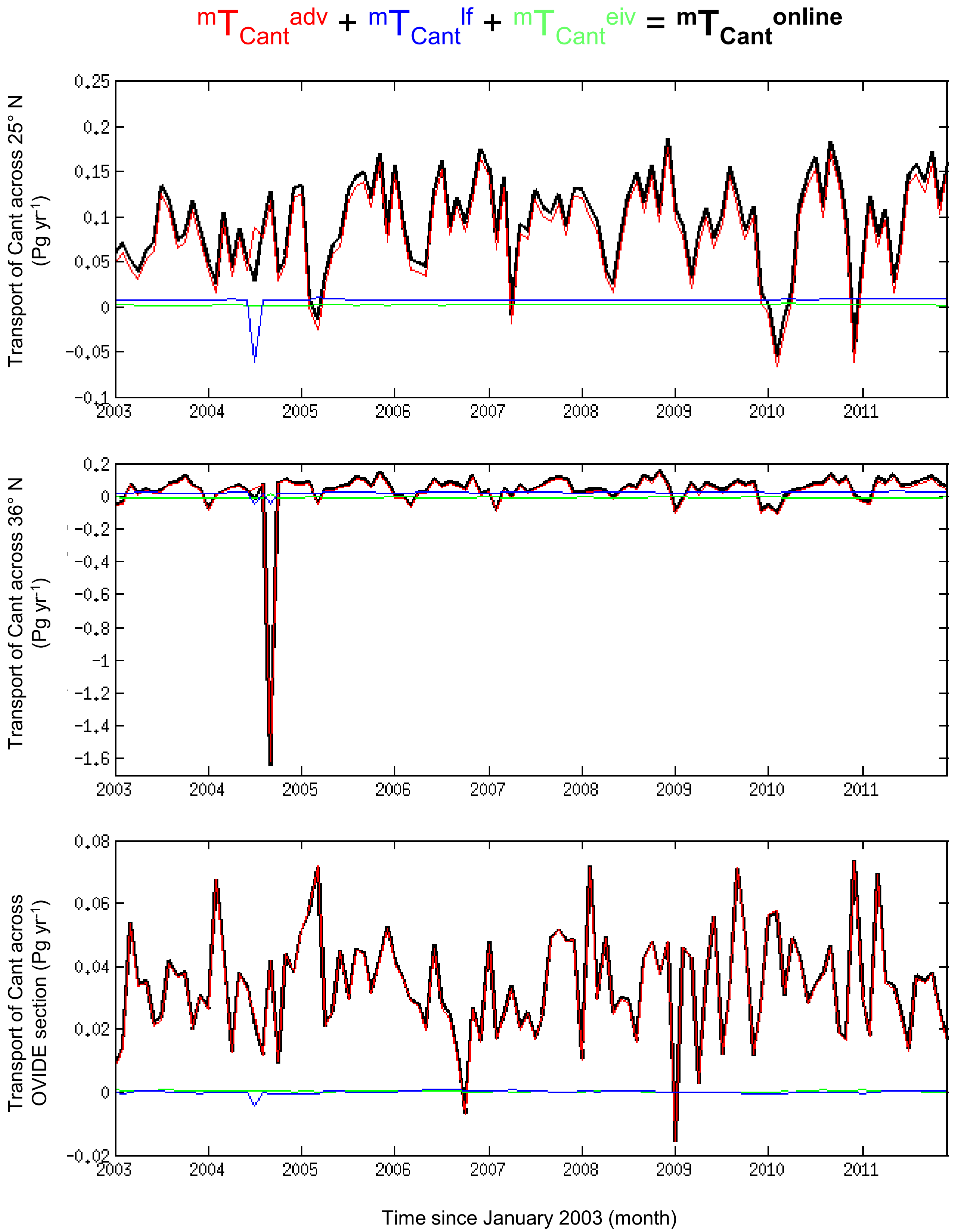

Fig. S3: Transport of Cant across (from top to bottom) 25° N, 36° N and OVIDE sections computed online by ORCA05-PISCES over the period 2003-2011 (monthly resolution). In the online approach, the transport of Cant (${}^{m}T_{Cant}{}^{online}$, black bold line) is the sum of the advection (${}^{m}T_{Cant}{}^{adv}$, red fine line), the diffusion (${}^{m}T_{Cant}{}^{lf}$, blue fine line) and the eddy (${}^{m}T_{Cant}{}^{eiv}$, green fine line) contribution. For each section, ${}^{m}T_{Cant}{}^{adv}$ is the major component of ${}^{m}T_{Cant}{}^{online}$.

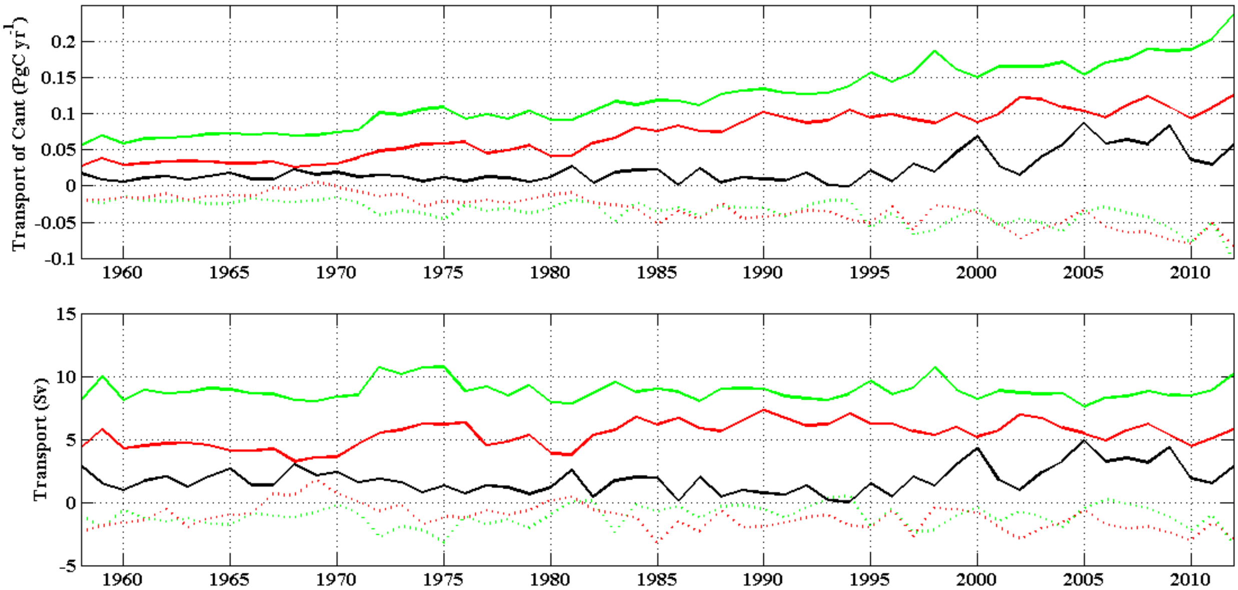

Fig S4a: Simulated annual time series of Cant and volume transported (Pg yr^{-1}) by the northward (full line) and southward (dashed line) following components of NACW (class 1) through 25°N (green), 36°N (red) and OVIDE (black) over the period 1959-2011.

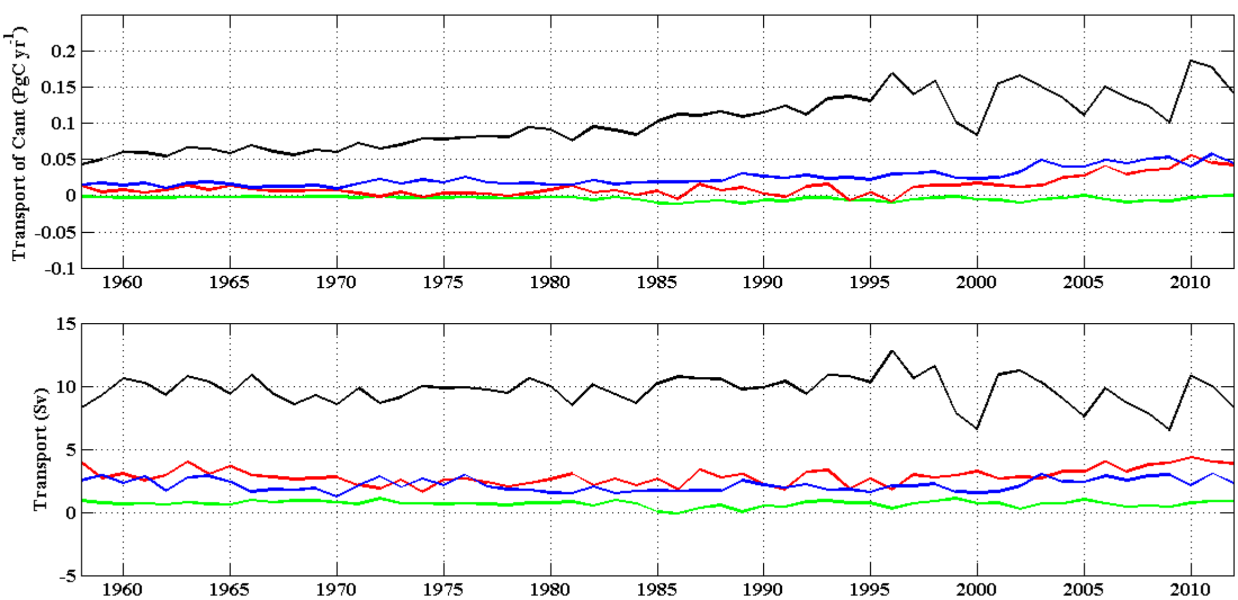

Fig S4b: : Simulated annual time series of Cant and volume transported (Pg yr^{-1}) within IW (class 2) through 25°N (green), 36°N (red), OVIDE (black) and the Greenland-Iceland-Scotland sills (blue) over the period 1959-2011.

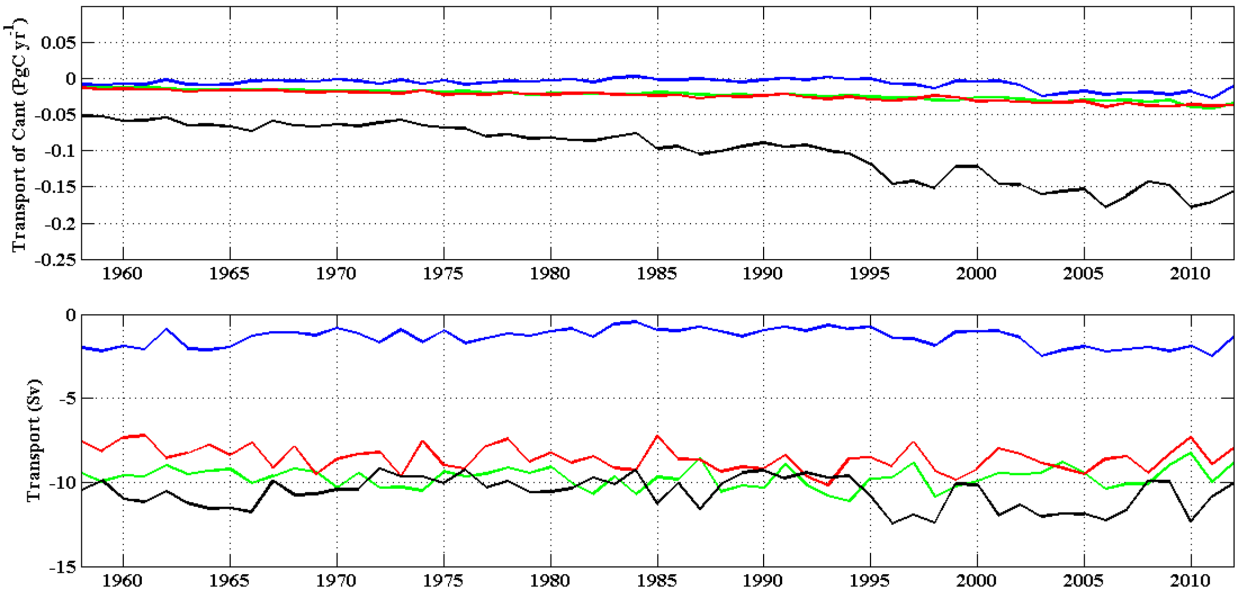

Fig S4c: : Simulated annual time series of Cant and volume transported (Pg yr^{-1}) within NADW (Class 3) through 25°N (green), 36°N (red), OVIDE (black) and the Greenland-Iceland-Scotland sills (blue) over the period 1959-2011.